PAPER

Check for updates

Revised values for the X23 benchmark set of molecular crystals†

Grygoriy A. Dolgonos, ‡ Johannes Hoja * and A. Daniel Boese *

We present revised reference values for cell volumes and lattice energies for the widely used X23 benchmark set of molecular crystals by including the effect of thermal expansion. For this purpose, thermally-expanded structures were calculated *via* the quasi-harmonic approximation utilizing three dispersion-inclusive density-functional approximations. Experimental unit-cell volumes were back-corrected for thermal and zero-point energy effects, allowing now a direct comparison with lattice relaxations based on electronic energies. For the derivation of reference lattice energies, we utilized harmonic vibrational contributions averaged over four density-functional approximations. In addition, the new reference values also take the change in electronic and vibrational energy due to thermal expansion into account. This is accomplished by either utilizing experimentally determined cell volumes and heat capacities, or by relying on the quasi-harmonic approximation. The new X23b reference values obtained this way will enable a more accurate benchmark for the performance of computational methods for molecular crystals.

Introduction

Computational and theoretical chemistry has come a long way: whereas physics already became more and more of theoretical nature with the advent of quantum mechanics at the beginning of the last century, chemistry has undergone an increased transformation towards theory only within the last twenty to thirty years. The methods regularly used[1,2] are classical *ab initio* methods, starting from a Hartree–Fock reference function, density functional theory (DFT), or semi-empirical methods which serve as an approximation to either one of the two families of methods.

Post-Hartree–Fock methods are nowadays able to predict properties of molecular systems up to virtually any desired accuracy by systematically improving the correlation treatment together with the wave function representation. Unfortunately, the computational time required by these methods scales conventionally with n to the power of five or higher – with n being the number of electrons. However, there are many recent efforts to make methods such as coupled cluster with single, double, and perturbative triple excitations [CCSD(T)] inherently linear scaling.[3–9] Still, important features such as analytical

gradients for geometry optimizations are not yet available for these linear scaling methods. This implies that, even with computers getting much faster, we cannot calculate the properties of much larger systems.

For DFT methods, it is much easier to achieve inherent near-linear scaling.[10–16] However, at this point there is a consensus that for DFT, while formally exact, an exact universal functional will not be available. This implies that the possibility for systematically improving DFT is missing, and convergence towards the highest accuracy can never be achieved. Finally, semi-empirical[17,18] and density-functional tight-binding[19] methods, which are even faster than DFT, are parameter dependent, have a smaller range of applicability, and are usually less accurate.

The situation is further complicated by the fact that for "periodic lattice problems", post-Hartree–Fock methods are still under development[20–23] and the computation with the so-called "gold standard" of quantum chemistry, CCSD(T), is not possible. Thus, until today, only DFT is commonly applied to predict solid-state properties of periodic systems such as molecular crystals. This directly implies that there is a lack of highly accurate reference values for periodic systems. Thus, for now such data has to be taken from experiment rather than computed with higher-level methods, introducing numerous deviations which can be found when comparing an experiment at finite temperature to an idealised model system within a computational model.

One of the main applications of the computational modelling of molecular crystals is organic crystal structure prediction. Therein, the goal is to predict the crystal-packing arrangement

Institute of Chemistry, University of Graz, Heinrichstraße 28/IV, 8010 Graz, Austria. E-mail: Adrian_Daniel.Boese@uni-graz.at, johannes.hoja@uni-graz.at

† Electronic supplementary information (ESI) available: Additional tables with calculated structural and thermodynamic quantities for all systems of the X23 data set. See DOI: 10.1039/c9cp04488d

‡ Current address: Institute of Solid State Physics, Graz University of Technology, Petersgasse 16, 8010 Graz, Austria.

This journal is © the Owner Societies 2019

Phys. Chem. Chem. Phys., 2019, **21**, 24333–24344 | 24333

occurring in crystallization experiments solely based on the structural formula of the involved chemical unit. This is primarily achieved by calculating a thermodynamic stability ranking of a vast number of different possible structures. Many molecular crystals can crystallise in more than one crystal-packing arrangement or polymorph and their stabilities typically differ by only very few kJ mol^{-1}.[24] Therefore, very accurate relative polymorph stabilities would be needed in order to confidently describe polymorphic systems. The success of crystal-structure-prediction methods in predicting the correct polymorph structure of a molecular crystal among the thermodynamically most-stable structures was evaluated in several blind tests organized by the Cambridge Crystallographic Data Centre.[25–30] However, these blind tests do not provide a direct benchmark for the accuracy of lattice energies.

Currently, the most used benchmark set for lattice energies, which compiles a diverse set of experimentally well determined molecular crystals, is the so-called X23 dataset of Reilly and Tkatchenko.[31] It extended upon the C21 set of Otero-de-la-Roza and Johnson[32] and contains 23 rather small molecular crystals with rather rigid molecules (see Fig. 1). Therein, the reference values are experimentally measured sublimation enthalpies, which have been back-corrected for vibrational contributions—allowing a direct benchmark of static lattice energies. The vibrational contributions in ref. 31 were obtained by using the harmonic approximation, which allows a computationally affordable determination of vibrational (free) energies using electronic structure methods but ignores all anharmonic effects.

However, the unit cell of molecular crystals expands with increasing temperature and several properties are highly volume dependent.[33] Vibrational contributions in the harmonic approximation are calculated at the minimum of the electronic energies. Hence, the used structures do not include any temperature effects, not even volumetric changes due to zero-point motion at a temperature of 0 K. The thermal expansion of a periodic system can be estimated *via* the so-called quasi-harmonic approximation (QHA), which has been recently used by several groups to study molecular crystals (including the original C21 publication).[32–44]

As new methods and density functionals are often developed by especially comparing to the X23 set of molecular crystals, improved reference values are direly needed going beyond the harmonic approximation for both lattice energies as well as cell volumes, even if they have been determined at low temperatures. In this contribution, we will address the effect of thermal expansion by utilizing dispersion-inclusive density functional theory.

First, we present new reference values for unit-cell volumes, which have been back-corrected for thermal expansion and zero-point vibrational effects in order to allow a direct benchmark of optimized structures at the minimum of the electronic energy. Second, we also present new reference values for lattice energies with harmonic vibrational contributions averaged over several density functional approximations, which minimizes the bias towards a certain density functional. Furthermore, we also discuss the effect of expansion on the lattice energies.

Computational methods

Calculation of crystal structures

Lattice relaxations. We performed full lattice and geometry relaxations for all molecular crystals within the X23 benchmark set[31] utilizing three commonly used density-functional approximations at the generalized-gradient level: PBE,[45] BLYP,[46,47] and RPBE.[48] The atom-pairwise D3 dispersion correction of Grimme[49]—utilising the Becke–Johnson damping function[50–54]—was applied throughout and the resulting methods are denoted as PBE+D3, BLYP+D3, and RPBE+D3.

All calculations were performed using the Vienna Ab Initio Simulation Package[55–58] (VASP, version 5.4.1) in a similar manner as reported in our earlier publications.[59,60] In all cases, the hard projector augmented-wave pseudopotentials[61,62] were used along an energy cut-off of 1000 eV. The convergence criteria for the periodic structure relaxation correspond to 10^{-5} eV for the energy and to 5×10^{-3} eV Å^{-1} for the gradient. All optimizations were carried out using the so-called "standard" k-point grid defined in ref. 60. These fully relaxed structures are referred to as V_{el}, indicating that the unit-cell volume corresponds to the minimum of the electronic energy.

Quasi-harmonic thermal expansion. Next, we included the effect of volumetric expansion due to zero-point and thermal effects in our description of molecular crystal structures *via*
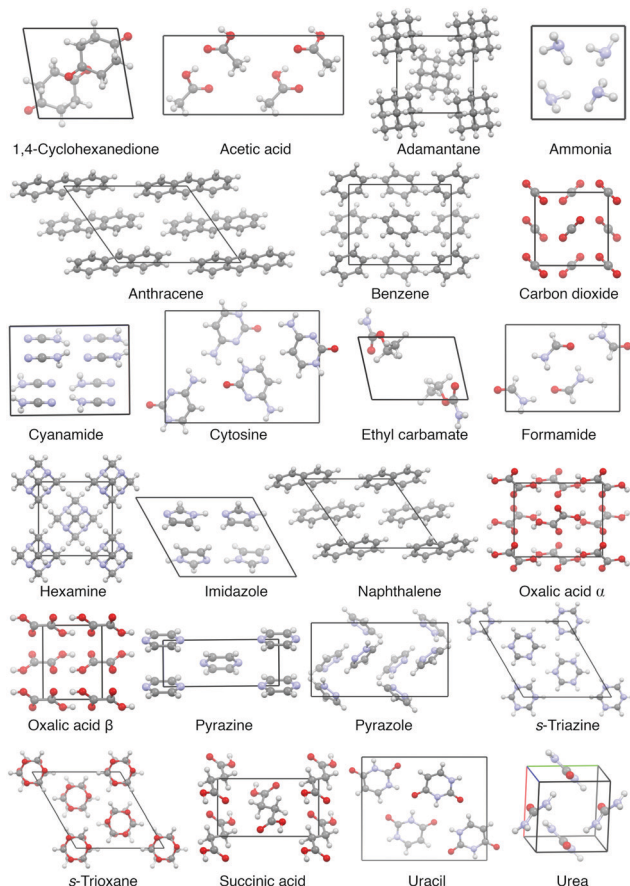

Fig. 1 Unit cells of all molecular crystals within the X23 dataset.

24334 | *Phys. Chem. Chem. Phys.*, 2019, **21**, 24333–24344

This journal is © the Owner Societies 2019

the QHA. Therein, vibrations of a particular geometry are still described in a harmonic fashion, but several different unit-cell volumes V are considered. The resulting Gibbs free energy $G(T,p)$ at a temperature T and a pressure p is given by

$$G(T, p) = \min_V [E_{el}(V) + F_{vib}(T, V) + pV], \qquad (1)$$

with $E_{el}(V)$ being the electronic energy at a certain unit-cell volume, which includes also the nuclear repulsion term. The vibrational free energy $F_{vib}(T,V)$ is derived from the standard harmonic oscillator vibrational partition function as obtained from statistical thermodynamics:

$$F_{vib}(T, V)$$
$$= \frac{1}{q_{total}} \sum_q^{q_{total}} \sum_i^{3N} \left\{ \frac{\hbar \omega_{q,i}(V)}{2} + k_B T \ln \left[1 - \exp \left(-\frac{\hbar \omega_{q,i}(V)}{k_B T} \right) \right] \right\},$$
$$(2)$$

with q_{total} being the total number of q-points used, N the number of atoms in the unit cell, k_B the Boltzmann constant, $\hbar$ the reduced Planck constant, while $\omega_{q,i}$ describes the harmonic vibrational frequency of mode i at q-point q.

One way of obtaining the volume corresponding to a certain temperature is the usage of a Murnaghan equation-of-state (EOS) fit,[63] as discussed in ref. 33. This requires the calculation of at least four vibrational free energies for different unit-cell volumes.

However, at zero temperature and by neglecting zero-point-energy effects, $G(T,p)$ can easily be minimised by applying an external hydrostatic pressure during the cell relaxation. Throughout, we are investigating molecular crystals at ambient pressure. This makes the effect of the pV term on the unit-cell volumes negligible. Relaxations under an external pressure can be utilised to efficiently mimic thermal (vibrational) effects.[32] The so-called thermal pressure p_{th} related to the effect of F_{vib} at a temperature T can be calculated according to

$$p_{th} = -\frac{dF_{vib}(T, V)}{dV}. \qquad (3)$$

The thermal expansion of the unit cell can then be modelled *via* a cell relaxation under a negative hydrostatic pressure of $-p_{th}$. The thermal pressure p_{th} was evaluated through numerical differentiation of F_{vib} *vs.* volume at the respective temperature of the experimental crystal-structure determination for all three density functional approximations. For this purpose, F_{vib} was calculated for unit cells, which were isotropically expanded and shrunk in terms of volume by 5% compared to their V_{el} and subsequently relaxed in terms of atomic positions. The respective thermal pressure was then obtained *via* a central finite difference and subsequently used for a lattice relaxation under an external pressure. Note that this approach requires only two vibrational free energy calculations for every system and allows for an anisotropic volumetric expansion. These relaxations lead to thermally expanded unit cells corresponding to the experimental structure determinations (between 2 K and 295 K) and these unit-cell volumes are referred to as V_l^{QHA}. Whenever available, low-temperature crystal-structure determinations with X-ray or neutron diffraction were used as experimental reference with

volume V_l^{exp} (see Table S1 in the ESI† for more details). Since we prefer not to alter the X23 dataset, we have always used the same polymorph as described in ref. 31. Note that a lower-temperature polymorph than the one used herein exists for *s*-triazine[64] below 198 K under ambient pressure. In addition, a small lambda-type phase transition at 96 K was observed for pyrazine,[65] suggesting a possible low-temperature polymorph. The new reference cell volumes corresponding to the electronic energy surface V_{el}^{ref} were then obtained *via*

$$V_{el}^{ref} = V_l^{exp} - \Delta V_l^{QHA}, \qquad (4)$$

with ΔV_l^{QHA} being the average of $V_l^{QHA} - V_{el}$ over all three used density functionals.

All periodic harmonic vibrational free energies were calculated *via* the finite displacement approach utilizing Phonopy.[66] These calculations were performed by using supercells with minimal lengths larger than 12 Å, finite displacements of 0.01 Å, and a $1 \times 1 \times 1$ k-grid. In contrast to geometry optimizations, these energy calculations were converged to 10^{-8} eV; all other VASP settings remain the same. The vibrational free energies were then evaluated within Phonopy using a $8 \times 8 \times 8$ q-point mesh. At the Γ-point, no actual imaginary modes were present and the magnitude of the three acoustic modes was always smaller than 3 cm^{-1}, and for every system except acetic acid even smaller than 1 cm^{-1}. For all optimizations under an external hydrostatic pressure $(-p_{th})$, gradients were converged to 2.5×10^{-3} eV Å^{-1}.

For PBE+D3 we have also explored the role of different numerical differentiation procedures (see Table S2, ESI†) and super cell sizes (see Table S3, ESI†) on the obtained thermal pressure values. The resulting thermal pressure differences are not significant—leading in the worst case to a modification of the cell volume by only 0.5% compared to our standard approach. In addition, we have also calculated the unit cells corresponding to a temperature of 0 K with PBE+D3 by taking into account zero-point vibrational energies.

Since we want to discuss sublimation enthalpies at mostly room temperature later on, we have also calculated with PBE+D3 high-temperature unit cells *via* the QHA with volumes V_h^{QHA} corresponding to a temperature of 298 K in most cases. For the systems for which a solid phase at 298 K at ambient pressure does not exist, the temperature of the corresponding melting point/triple point[67–70] was used (see Table S1, ESI†); in the case of carbon dioxide, the used temperature corresponds to the sublimation enthalpy measurement[71] at the highest available temperature (207 K), since no local minimum can be found at larger thermal pressures.

Experimental unit-cell volumes. Moreover, high-temperature unit cells corresponding to experimentally determined volumes V_h^{exp} were obtained *via* constrained-volume optimizations by using PBE+D3 (see Table S1, ESI†). For the three systems without an available high-temperature experimental volume, V_h^{exp} was approximated by

$$V_h^{exp} = V_l^{exp} + V_h^{QHA} - V_l^{QHA}. \qquad (5)$$

This way, we rely on the available experimental low-temperature structure and add our calculated thermal expansion between T_l and 298 K according to the QHA.

Calculation of sublimation enthalpies

Harmonic approximation. The enthalpy of sublimation (ΔH_{sub}) is defined as the enthalpy difference between the gaseous molecule (H_{gas}) and the crystal (H_{cr}), divided by the number of molecules per unit cell, n:

$$\Delta H_{sub} = H_{gas} - \frac{H_{cr}}{n} \qquad (6)$$

Note that the sublimation enthalpy does not contain any entropic effects. The absolute enthalpy of a molecule H_{gas} was calculated under the ideal gas approximation as the sum of its electronic energy ($E_{el,g}$) and respective terms corresponding to its translational, rotational, and vibrational degrees of freedom ($E_{vib,g}$), as well as a pV term:

$$H_{gas} = E_{el,g} + \frac{3}{2}RT + \frac{3}{2}RT + E_{vib,g} + RT \qquad (7)$$

For non-linear molecules the translational and rotational contribution amounts in both cases to $(3/2)RT$, with R being the gas constant. For linear molecules (like carbon dioxide) the rotational contribution amounts to only RT within the ideal gas approximation, $pV = RT$. The vibrational internal energy $E_{vib,g}$ was calculated according to

$$E_{vib,g} = \sum_{i=1}^{m} \left[\frac{\hbar\omega_i}{2} + \frac{\hbar\omega_i}{\exp\left(\frac{\hbar\omega_i}{k_B T}\right) - 1} \right], \qquad (8)$$

with $m = 3N - 6$ and $m = 3N - 5$ for non-linear and linear molecules, respectively.

The enthalpy of the crystal H_{cr} consists of three terms: the electronic energy $E_{el,cr}$, the vibrational internal energy $E_{vib,cr}$ and a pV term:

$$H_{cr} = E_{el,cr} + E_{vib,cr} + pV \qquad (9)$$

The pV term under standard conditions contributes only less than 0.05 kJ mol^{-1} to the crystal enthalpy H_{cr} of any of the studied crystals and was therefore neglected. The vibrational energy contribution of a periodic system $E_{vib,cr}$ is calculated according to:

$$E_{vib,cr} = \frac{1}{q_{total}} \sum_{q}^{q_{total}} \sum_{i}^{3N} \left[\frac{\hbar\omega_{q,i}}{2} + \frac{\hbar\omega_{q,i}}{\exp\left(\frac{\hbar\omega_{q,i}}{k_B T}\right) - 1} \right], \qquad (10)$$

with q_{total} being the total number of q-points q. The difference between the vibrational internal energy of a gas-phase molecule and a crystal (normalized per molecule) at a given temperature corresponds to

$$\Delta E_{vib} = E_{vib,g} - \frac{E_{vib,cr}}{n}. \qquad (11)$$

Therefore, the sublimation enthalpy ΔH_{sub} can now be calculated according to

$$\Delta H_{sub} = \left(E_{el,g} - \frac{E_{el,cr}}{n} \right) + \Delta E_{vib} + 4RT$$
$$= E_{latt} + \Delta E_{vib} + 4RT, \qquad (12)$$

where E_{latt} stands for the lattice energy of a crystal. In this definition E_{latt} is positive and refers to the energy needed for the infinite separation of molecules. Note that for the linear molecule carbon dioxide the last term amounts here and in subsequent equations to $3.5RT$.

We have calculated the sublimation enthalpies of all X23 systems with PBE+D3, BLYP+D3, and RPBE+D3 at temperatures T_h^{calc} (mostly 298 K, see Table S1, ESI†) using the respective fully optimized structures (at V_{el}). The periodic vibrational internal energies were calculated using Phonopy as described above. All molecular DFT calculations were performed in an empty periodic box of 17 Å in each dimension using VASP. The gas phase molecular structure was in most cases obtained by optimizing the molecular structure of the crystalline phase. However, in the case of oxalic acid we used a conformation with an intramolecular hydrogen bond, since this is significantly more stable than any conformation without a hydrogen bond. For succinic acid, we used a *gauche* conformer corresponding to conformer I in ref. 72. The molecular vibrational modes were calculated directly using VASP.

Based on the harmonic vibrational energies obtained this way, we have derived new reference values for lattice energies ($E_{latt}^{ref,HA}$) according to

$$E_{latt}^{ref,HA} = \Delta H_{sub}^{exp} - (\Delta E_{vib}^{avg} + 4RT), \qquad (13)$$

where ΔE_{vib}^{avg} is the average over ΔE_{vib} calculated with PBE+D3, BLYP+D3, RPBE+D3, and the PBE+TS[73] values from ref. 31. For all systems with $T_h^{calc} < 298$ K, the average was only calculated using the three DFT+D3 approaches. The term ΔH_{sub}^{exp} denotes the experimental sublimation enthalpy.

For systems with $T_h^{calc} = 298$ K, we used the ΔH_{sub}^{exp} values listed in ref. 31 except for naphthalene[74] and cytosine.[75] For the five systems where $T_h^{calc} < 298$ K, the ΔH_{sub}^{exp} values were obtained as follows: for ammonia, carbon dioxide, and formamide we used the experimental value closest to T_h^{calc} listed in ref. 76; for benzene we used the average of experimental values in ref. 76 within 5 K of T_h^{calc}; for acetic acid we extrapolated both values listed in ref. 76 to 290 K *via* eqn (3) therein using the experimentally determined heat capacity from ref. 77. Adamantane shows at 208 K a phase transition from the here considered tetragonal polymorph to a cubic polymorph, which is accounted for by adding the enthalpy of the phase transformation (3.2 kJ mol^{-1}) to ΔH_{sub}^{exp}.[78]

Quasi-harmonic approximation. Furthermore, we investigated the effect of thermal expansion on the reference lattice energies by calculating the vibrational energies with PBE+D3 at T_h^{calc} using the respective thermally expanded structures at V_h^{QHA}. Subsequently, we have compared the results with the ones obtained at V_{el}; the lattice energy difference is expressed

24336 | *Phys. Chem. Chem. Phys.,* 2019, **21**, 24333–24344

This journal is © the Owner Societies 2019

as $\Delta\Delta E_{\text{latt}}^{\text{QHA}}$, while the difference in vibrational energies is labelled $\Delta\Delta E_{\text{vib}}^{\text{QHA}}$. The total effect of the QHA is captured by $\Delta\Delta E_{\text{sub}}^{\text{QHA}}$, which is the sum of the two terms described above. This allows us to derive another set of reference lattice energies $E_{\text{latt}}^{\text{ref,QHA}}$, which back-corrects also for thermal expansion effects on the quasi-harmonic level:

$$E_{\text{latt}}^{\text{ref,QHA}} = E_{\text{latt}}^{\text{ref,HA}} - \Delta\Delta E_{\text{latt}}^{\text{QHA}} - \Delta\Delta E_{\text{vib}}^{\text{QHA}} = E_{\text{latt}}^{\text{ref,HA}} - \Delta\Delta E_{\text{sub}}^{\text{QHA}}. \quad (14)$$

Experimental volumes and heat capacities. Finally, we have created another set of reference lattice energies by taking additional experimental measurements into account. For this purpose, we have calculated lattice energies and vibrational energies at $T_{\text{h}}^{\text{calc}}$ with PBE+D3 using the respective optimized structures at $V_{\text{h}}^{\text{exp}}$, which correspond (in most cases) to experimentally measured cell volumes at or close to $T_{\text{h}}^{\text{calc}}$ (see Table S1, ESI†). Furthermore, we also utilize (whenever available) experimentally measured heat capacities in a similar fashion as described by Reilly and Tkatchenko[31] (see Table S1, ESI†). The vibrational internal energy of the crystal $E_{\text{vib,cr}}$ can also be expressed as

$$E_{\text{vib,cr}} = E_{\text{ZPE}} + \int_0^T C_{\text{p}} dT, \quad (15)$$

where E_{ZPE} describes the zero-point energy and C_{p} describes the heat capacity at constant pressure. Whenever experimental C_{p} values were available for the entire needed temperature range, $E_{\text{vib,cr}}$ was obtained via PBE+D3 zero-point energies at $V_{\text{h}}^{\text{exp}}$ and the numeric integration over experimental C_{p} values. In cases for which these experimental values were not available below 15 K or for temperatures close to $T_{\text{h}}^{\text{calc}}$, we used quasi-harmonic PBE+D3 results for the missing temperature range, while experimental values were used for the remainder (see Table S1, ESI†). The quasi-harmonic C_{p} values[79] were obtained via

$$C_{\text{P}} = -T\frac{\partial^2 G}{\partial T^2} \quad (16)$$

utilizing an EOS fit within phonopy. For the EOS fit, we used the available PBE+D3 free energies calculated at V_{el}, $V_{\text{h}}^{\text{QHA}}$, and at the isotropically expanded/shrunk cell volumes $0.9V_{\text{el}}$, $0.95V_{\text{el}}$, and $1.05V_{\text{el}}$. Since the QHA significantly overestimates the thermal expansion of carbon dioxide at higher temperatures (see below), the corresponding C_{p} values were approximated by simply adding R to the harmonic heat capacity at constant volume C_{V} ($V_{\text{h}}^{\text{exp}}$), which corresponds to the ideal gas approximation. C_{V} can be obtained via

$$C_{\text{V}} = \frac{1}{q_{\text{total}}} \sum_q^{q_{\text{total}}} \sum_i^{3N} k_{\text{B}} \left(\frac{\hbar\omega_{q,i}}{k_{\text{B}}T}\right)^2 \frac{\exp\left(\frac{\hbar\omega_{q,i}}{k_{\text{B}}T}\right)}{\left[\exp\left(\frac{\hbar\omega_{q,i}}{k_{\text{B}}T}\right) - 1\right]^2}. \quad (17)$$

For oxalic acid β and pyrazole, no experimental heat capacities could be found and, therefore, quasi-harmonic C_{p} values were used for the entire temperature range.

The resulting reference energies $E_{\text{latt}}^{\text{ref,exp}}$ were then obtained via

$$E_{\text{latt}}^{\text{ref,exp}} = E_{\text{latt}}^{\text{ref,HA}} - \Delta\Delta E_{\text{latt}}^{\text{exp}} - \Delta\Delta E_{\text{vib}}^{\text{exp}} = E_{\text{latt}}^{\text{ref,HA}} - \Delta\Delta E_{\text{sub}}^{\text{exp}}, \quad (18)$$

where the definition of the energy terms is analogous to that in eqn (14).

Results and discussion

Cell volumes

We start by investigating the volumetric expansion of all molecular crystals within the X23 data set[31] when anharmonic effects are considered within the quasi-harmonic approximation (QHA). Therefore, we have first calculated the respective thermal pressures p_{th} using PBE+D3, BLYP+D3, and RPBE+D3 (see Table 1). The used temperatures T_{l} correspond to the temperatures of the experimental crystal-structure determinations, preferably at low temperatures (see Table S1, ESI†).

The PBE+D3 and RPBE+D3 values are very similar, with a mean absolute relative deviation (MARD) of 7% and a maximum deviation of 24% (cyanamide). In contrast, BLYP+D3 yields significantly different thermal pressures than PBE+D3 with a MARD of 46%. For oxalic acid β and succinic acid, the BLYP+D3 thermal pressure is twice as large as the corresponding PBE+D3 value in both cases.

Our obtained thermal pressures are similar to the ones obtained by Otero-de-la-Roza and Johnson,[32] although the latter are often smaller. However, a direct comparison of thermal pressures obtained with different methods does not provide significant insight since the resulting thermal expansion highly depends on the potential energy surface corresponding to the utilized method. For instance, as discussed below, BLYP+D3 yields significantly larger thermal pressures than PBE+D3, but very similar changes in cell volumes. Therefore, thermal pressure differences between density functionals are to be expected and cell volume changes are in fact the more important quantity for comparisons.

Table 1 Obtained thermal pressures (in GPa) for several density-functional approximations at a given temperature T_{l} (in K). Reference values from ref. 32, which do not correspond to T_{l}, are omitted

System	T_{l}	PBE+D3	BLYP+D3	RPBE+D3	Ref. 32
1,4-Cyclohexanedione	133	0.439	0.569	0.427	0.275
Acetic acid	40	0.197	0.302	0.211	0.201
Adamantane	188	0.536	0.728	0.507	0.343
Ammonia	2	0.402	0.443	0.384	n/a
Anthracene	16	0.235	0.386	0.252	n/a
Benzene	4	0.235	0.370	0.262	n/a
Carbon dioxide	6	0.190	0.260	0.159	n/a
Cyanamide	108	0.151	0.279	0.187	0.095
Cytosine	295	0.487	0.667	0.476	0.294
Ethyl carbamate	168	0.412	0.523	0.395	0.331
Formamide	90	0.324	0.436	0.319	0.137
Hexamine	15	0.310	0.462	0.317	n/a
Imidazole	123	0.191	0.354	0.185	0.267
Naphthalene	10	0.236	0.382	0.254	0.215
Oxalic acid α	295	0.628	0.753	0.601	0.496
Oxalic acid β	295	0.285	0.570	0.321	0.510
Pyrazine	184	0.472	0.594	0.461	0.252
Pyrazole	108	0.268	0.373	0.283	0.316
s-Triazine	295	0.740	0.878	0.738	0.531
s-Trioxane	103	0.426	0.549	0.397	0.661
Succinic acid	77	0.184	0.386	0.201	n/a
Uracil	295	0.388	0.480	0.439	0.398
Urea	12	0.374	0.461	0.389	n/a

All thermal pressures in Table 1 approximate vibrational-free energy effects at the minimum of the electronic energy (V_{el}) and have been obtained in a cost-effective way *via* central finite differences using two unit cells with volumes of $0.95V_{el}$ and $1.05V_{el}$, respectively. For PBE+D3 we have also investigated other schemes for determining the thermal pressure based on central, backward, and forward finite differences (see Table S2, ESI†).

From the ESI,† it can be seen that the central difference approach already yields accurate results since the addition of another two data points does not change the corresponding thermal pressure. Backward differences yield similar data in many cases and on average the thermal pressures are about 2% smaller.

For pyrazole and *s*-triazine, we have also calculated the thermal pressures at $1.05V_{el}$ utilizing central differences, resulting in slightly smaller thermal pressures compared to those listed in Table 1. For pyrazole, this thermal pressure difference leads to a modification of the unit-cell volume of 0.4%. While that modification is small, this approach might be more exact since we can expect a volumetric expansion of about 5% on average (see below).

In addition, we have also investigated the usage of larger supercells modifying the derived thermal pressures (see Table S3, ESI†). On average, the obtained thermal pressures change by 2.5% and the observed maximal difference was found to be 9% for uracil—leading to an alteration of the unit-cell volume by only 0.5%. Using larger supercells changes the vibrational free energy by only 0.1 kJ mol^{-1} on average and the largest observed difference amounts to 0.4 kJ mol^{-1} for cytosine. Therefore, our standard supercells provide sufficiently accurate results.

Furthermore, we have also validated the quality of the used thermal-pressure optimization by comparing with EOS fits. The comparison was performed for all systems with T_l other than room temperature utilizing the available PBE+D3 phonon calculations at V_{el}, V_h^{QHA} and the isotropically expanded/shrunk cell volumes of $0.9V_{el}$, $0.95V_{el}$, and $1.05V_{el}$. The average difference in the resulting unit-cell volumes between the thermal pressure and EOS approaches amounts to only 0.3%, with a mean absolute difference of 0.4%, while all differences are smaller than 0.8%.

Note that the deviation between thermal pressure optimizations and EOS fits will likely increase with temperature since our derived constant thermal pressure corresponds to V_{el}. Therefore, evaluating the thermal pressure close to the expected thermally-expanded volume should provide better results at high temperatures.

Next, we discuss the resulting volumetric expansions of the unit cells. This expansion includes thermal effects as well as zero-point energy effects. Fig. 2 shows the obtained expansions in % for all three density-functional approximations and the blue dashed line indicates the average expansion from 2 K to 295 K.

The numeric data compared to several literature values is available in Table S4 (ESI†). All resulting cell volumes are listed in Tables S5 and S6 (ESI†) contains all cell parameters for PBE+D3-optimised structures at V_{el} and V_l^{QHA}. The RPBE+D3 result for pyrazole was omitted in Fig. 2 and in the discussion later on due to an unrealistically large volumetric expansion of 27%. Based on all shown data points, the average expansion
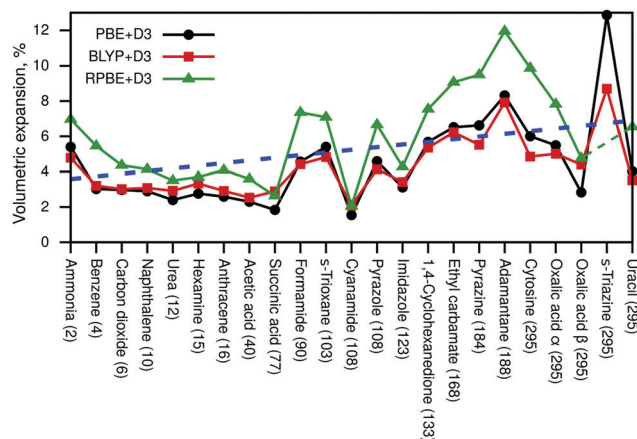

Fig. 2 Volumetric expansion due to zero-point and thermal effects (in %) of all studied molecular crystals calculated with PBE+D3, BLYP+D3, and RPBE+D3 compared to V_{el}. The considered temperatures are given for each crystal in parentheses and correspond to the temperature of the available experimental crystallographic measurements. The RPBE+D3 result for *s*-triazine was omitted due to an unrealistically large thermal expansion. The blue dashed line indicates a linear trend of thermal expansion w.r.t. temperature calculated using all shown data points. Note that the blue dashed line corresponds to 2 K at the first point on the *x*-axis and to 295 K at the last point on the *x*-axis.

amounts to about 5%, while a linear fit (blue line) suggests that the expansion due to zero-point fluctuations amounts to about 3.6% and that thermal effects lead additionally to a percentage expansion of $0.01T$. The volumetric expansion due to zero-point effects (at 0 K) was explicitly calculated with PBE+D3, leading to an average expansion of 2.4%.

It can be seen in Fig. 2 that PBE+D3 and BLYP+D3 yield very similar values for the volumetric expansion despite their differences in p_{th}, while RPBE+D3 yields significantly larger values.

Moreover, we have compared our results with force-field data (FIT, W99rev6311P5) from Nyman *et al.*[80] (see Table S4, ESI†). Unfortunately, the force-field results are quite scattered; several values are smaller than our DFT data, while some are significantly larger. In addition, the FIT force field yields even an unphysical negative volumetric expansion for cyanamide, suggesting that force fields might not be robust enough to properly deal with certain molecular crystals. Furthermore, our calculated values (especially PBE+D3 and BLYP+D3) agree very well with post-Hartree–Fock data from ref. 42 (acetic acid, carbon dioxide, imidazole).

Based on the obtained volumetric expansions corresponding to a temperature T_l, we can now provide a back-correction for experimental unit-cell volumes. The resulting reference values can then be directly compared with lattice relaxations minimising the electronic energy. Since the QHA works best at low temperatures due to minimal anharmonic effects, low-temperature experimental volumes were used when available. The average expansion of all three methods is used for the back-correction in order to minimize the influence of a single density functional. Note that a similar back-correction was presented for X23 in ref. 60 using the force-field data from Nyman *et al.*[80]

24338 | *Phys. Chem. Chem. Phys.*, 2019, **21**, 24333–24344

This journal is © the Owner Societies 2019

Table 2 Experimental cell volumes V_l^{exp} at temperatures T_l and new, final electronic reference volumes V_{el}^{ref} according to eqn (4). The listed uncertainties correspond to the maximal difference of individual V_l^{QHA} values (PBE+D3, BLYP+D3, RPBE+D3) from their average value for every system

System	T_l/K	V_l^{exp}/Å^3	V_{el}^{ref}/Å^3
1,4-Cyclohexanedione	133	279.6	262.5 ± 4.2
Acetic acid	40	297.3	288.8 ± 2.7
Adamantane	188	393.1	357.6 ± 10.6
Ammonia	2	128.6	121.5 ± 1.7
Anthracene	16	455.2	441.2 ± 4.0
Benzene	4	461.8	444.3 ± 7.1
Carbon dioxide	6	171.3	164.8 ± 2.1
Cyanamide	108	415.7	407.9 ± 1.4
Cytosine	295	472.4	440.3 ± 14.3
Ethyl carbamate	168	248.8	231.2 ± 4.9
Formamide	90	224.1	211.9 ± 4.7
Hexamine	15	332.4	321.6 ± 1.6
Imidazole	123	348.8	336.4 ± 2.7
Naphthalene	10	340.8	329.7 ± 2.6
Oxalic acid α	295	312.6	293.2 ± 6.1
Oxalic acid β	295	156.9	150.5 ± 1.9
Pyrazine	184	203.6	189.6 ± 4.8
Pyrazole	108	698.3	662.5 ± 11.3
s-Triazine	295	586.8	528.0 ± 12.8[a]
s-Trioxane	103	616.5	580.7 ± 9.6
Succinic acid	77	239.3	233.3 ± 1.5
Uracil	295	463.4	442.0 ± 8.9
Urea	12	145.1	140.8 ± 0.9

[a] RPBE+D3 result omitted due to unrealistically large thermal expansion.

Table 2 displays the final new electronic reference values V_{el}^{ref}. It can be seen that the values of V_{el}^{ref} are on average 5% smaller than the experimentally determined volumes. Since our back-correction utilizes the average over three methods, we also supply an uncertainty for the new reference values, which amounts to the maximal difference from the average value in both directions. On average, this uncertainty in the unit-cell volume amounts to about 1.5%. Note that these uncertainties do not include the experimental error. Since the deviation of available experimental unit-cell volumes for the X23 set corresponding to the same temperature is typically below 1%, we expect the experimental error to be less than our average calculated error of 1.5% for X23. For some other molecular crystals, the spread of experimentally determined cell volumes can be much larger. This is for instance illustrated in ref. 44 for paracetamol (acetaminophen).

Given the large effect of the back-correction, these new reference values should serve as new reference for benchmarking volumes obtained *via* minimization of electronic energies rather than the experimentally obtained cell volumes.

Lattice energies

After discussing cell volumes, we can turn to the calculation of new reference values for lattice energies. Reilly and Tkatchenko[31] have back-corrected experimental sublimation enthalpies by removing vibrational contributions calculated with PBE+TS in the harmonic approximation. In addition, they have provided so-called semi-anharmonic values for some systems by utilizing experimental heat capacities.

First, we discuss and compare our corresponding harmonic values calculated at V_{el}. Table 3 shows our $\Delta E_{vib} + 4RT$

Table 3 Vibrational contributions $\Delta E_{vib} + 4RT$ at temperatures T_h^{calc} (298 K unless stated otherwise) for several methods. PBE+TS values from ref. 31 are only available at 298 K and are therefore not listed if $T_h^{calc} < 298$ K. The first (or only) reported value refers to harmonic contributions while "semi-anharmonic" values reported in ref. 31 are listed after the slash. All values are given in kJ mol^{-1}

System	Ref. 31	PBE+D3	BLYP+D3	RPBE+D3
1,4-Cyclohexanedione	−7.5	−6.1	−7.9	−6.2
Acetic acid[a]	n/a	−4.3	−5.4	−4.9
Adamantane	−8.0/−11.0	−4.9	−8.3	−6.2
Ammonia[b]	n/a	−6.4	−7.0	−6.8
Anthracene	−7.6/−10.9	−6.3	−9.3	−6.7
Benzene[c]	n/a	−5.2	−6.7	−5.7
Carbon dioxide[d]	n/a	−2.7	−2.9	−2.8
Cyanamide	−4.2	−3.6	−4.6	−3.9
Cytosine	−6.4	−5.5	−7.3	−5.9
Ethyl carbamate	−7.6	−6.1	−7.6	−6.3
Formamide[e]	n/a	−6.9	−7.9	−7.3
Hexamine	−9.9/−10.4	−7.4	−9.4	−8.5
Imidazole	−5.5	−4.9	−6.2	−5.3
Naphthalene	−7.9/−10.5	−5.9	−8.2	−6.2
Oxalic acid α	−4.7	−2.3	−3.5	−3.2
Oxalic acid β	−2.4	−2.2	−3.9	−2.9
Pyrazine	−5.0	−6.3	−7.3	−6.3
Pyrazole	−5.4	−4.8	−6.1	−5.4
s-Triazine	−6.0	−5.4	−6.3	−5.6
s-Trioxane	−8.3/−10.1	−6.8	−8.2	−7.0
Succinic acid	−4.3/−7.2	−3.0	−5.7	−3.8
Uracil	−6.5	−5.6	−7.1	−6.0
Urea	−6.6/−8.7	−7.1	−7.9	−7.3

[a] $T = 290$ K. [b] $T = 195$ K. [c] $T = 279$ K. [d] $T = 207$ K. [e] $T = 276$ K.

contributions obtained with PBE+D3, BLYP+D3, and RPBE+D3 as well as the PBE+TS results from ref. 31. Since the experimental sublimation enthalpies are typically extrapolated to the standard temperature 298 K, we have evaluated the $\Delta E_{vib} + 4RT$ contributions in most cases at this temperature. However, for systems which do not exist in a solid form at 298 K, we have reduced the temperature (see T_h^{calc} in Table 4). For completeness, vibrational contributions at 298 K for structures with $T_h^{calc} < 298$ K are available in Table S7 (ESI†).

For our DFT+D3 vibrational contributions (Table 3), we observe the following general trend: PBE+D3 < RPBE+D3 < BLYP+D3. The mean absolute deviation (MAD) of PBE+D3, BLYP+D3, and RPBE+D3 compared to the harmonic PBE+TS values amounts to 1.3, 0.8, and 0.9 kJ mol^{-1}, respectively. Interestingly, PBE+D3 deviates the most from the PBE+TS results. All four methods show a good agreement with an average energy interval of 1.7 kJ mol^{-1}. The worst agreement is found for adamantane, for which the maximal difference between the discussed methods amounts to 3.4 kJ mol^{-1}—originating from the difference between the D3 and the Tkatchenko–Scheffler (TS) dispersion models.

Vibrational contributions turned out to be less pronounced for the small and rigid systems (*e.g.*, carbon dioxide, cyanamide and two oxalic acids polymorphs), for which the conformational difference of a molecule between the gas-phase and the solid state is negligible. On the contrary, larger, conformationally flexible, and mostly nitrogen-containing systems are prone to large vibrational contributions (*e.g.*, ammonia, urea, formamide, hexamine) on account of a different degree of planarization of

This journal is © the Owner Societies 2019

Phys. Chem. Chem. Phys., 2019, **21**, 24333–24344 | 24339

Table 4 Averaged harmonic vibrational contributions $\Delta E_{vib}^{avg} + 4RT$ at temperatures T_h^{calc} together with the terms $\Delta\Delta E_{sub}^{QHA}$ and $\Delta\Delta E_{sub}^{exp}$, which estimate anharmonic effects (see eqn (14) and (18)). The temperatures are given in K while all vibrational contributions are listed in kJ mol^{-1}

System	T_h^{calc}	$\Delta E_{vib}^{avg} + 4RT$	$\Delta\Delta E_{sub}^{QHA}$	$\Delta\Delta E_{sub}^{exp}$
1,4-Cyclohexanedione	298	−6.9	−3.1	−2.0
Acetic acid	290	−4.9	−1.2	−1.1
Adamantane	298	−6.9	−3.5	−3.4
Ammonia	195	−6.7	−0.1	−0.8
Anthracene	298	−7.5	−1.8	−1.0
Benzene	279	−5.9	−3.7	−4.0
Carbon dioxide	207	−2.8	−2.8	−0.5
Cyanamide	298	−4.1	−0.1	−1.9
Cytosine	298	−6.3	−0.6	−0.9
Ethyl carbamate	298	−6.9	−1.4	−2.6
Formamide	276	−7.4	−0.9	−2.1
Hexamine	298	−8.8	−2.2	0.5
Imidazole	298	−5.5	−0.5	−3.4
Naphthalene	298	−7.1	−2.7	−1.7
Oxalic acid α	298	−3.4	−0.8	−1.6
Oxalic acid β	298	−2.9	−0.1	−0.4
Pyrazine	298	−6.2	−1.9	−1.7
Pyrazole	298	−5.4	−1.7	−1.0
s-Triazine	298	−5.8	−2.7	−1.1
s-Trioxane	298	−7.6	−2.1	−0.8
Succinic acid	298	−4.2	−0.8	−2.8
Uracil	298	−6.3	−0.2	−0.7
Urea	298	−7.2	−0.9	−1.1

Table 5 Experimental sublimation enthalpies ΔH_{sub}^{exp} at temperatures T_h^{calc} (see Computational methods) together with the three derived sets of reference lattice energies ($E_{latt}^{ref,HA}$, $E_{latt}^{ref,QHA}$, $E_{latt}^{ref,exp}$) as defined by eqn (13), (14), and (18). The computational uncertainty of the new reference values Δ_{max} is always estimated by the maximal difference between the individual ΔE_{vib} values from ΔE_{vib}^{avg}. Note that Δ_{max} does not include any experimental uncertainty. All values are given in kJ mol^{-1}

System	ΔH_{sub}^{exp}	$E_{latt}^{ref,HA}$	$E_{latt}^{ref,QHA}$	$E_{latt}^{ref,exp}$	Δ_{max}
1,4-Cyclohexanedione	81.1	88.0	91.1	**90.0**	1.0
Acetic acid	67.7	72.6	73.7	**73.6**	0.6
Adamantane	61.6	68.5	71.9	**71.8**	2.0
Ammonia	31.2	37.9	38.1	**38.7**	0.3
Anthracene	101.9	109.4	111.2	**110.4**	1.8
Benzene	44.9	50.8	54.5	**54.8**	0.8
Carbon dioxide	26.1	28.9	31.7	**29.4**	0.1
Cyanamide	75.5	79.6	79.7	**81.5**	0.5
Cytosine	156.4	162.7	163.3	**163.5**	1.0
Ethyl carbamate	78.7	85.6	87.0	**88.2**	0.8
Formamide	71.7	79.1	80.0	**81.1**	0.5
Hexamine	75.8	84.6	86.8	**84.1**	1.4
Imidazole	81.4	86.9	87.4	**90.4**	0.7
Naphthalene	72.6	79.7	82.4	**81.3**	1.2
Oxalic acid α	93.7	97.1	97.9	**98.8**	1.3
Oxalic acid β	93.6	96.5	96.5	**96.8**	1.1
Pyrazine	56.3	62.5	64.4	**64.3**	1.2
Pyrazole	72.4	77.8	79.5	**78.8**	0.7
s-Triazine	55.7	61.5	64.2	**62.6**	0.5
s-Trioxane	56.3	63.9	66.0	**64.6**	0.8
Succinic acid	123.1	127.3	128.0	**130.1**	1.5
Uracil	129.2	135.5	135.7	**136.2**	0.8
Urea	93.8	101.0	102.0	**102.1**	0.7

nitrogen atoms in the crystal compared to that in the gas phase. Based on the average of the PBE+TS, PBE+D3, BLYP+D3, and RPBE+D3 results ($\Delta E_{vib}^{avg} + 4RT$), we derive new harmonic reference values for lattice energies ($E_{latt}^{ref,HA}$), which are listed in Table 5. Using the average over four methods should minimize the bias of the reference values towards a single density functional. The MAD between the ΔE_{vib} terms and the harmonic PBE+TS results from Ref. 31 amounts to 0.5 kJ mol^{-1}, with a maximum difference of 1.3 kJ mol^{-1} (oxalic acid α).

As estimated uncertainty Δ_{max} for our calculated reference values, we utilize the maximal difference between a specific method and the average ΔE_{vib}^{avg}. Note that this error estimation does not include any error of the underlying experimental reference data. Estimating the experimental error of sublimation enthalpies is a non-trivial task. Here, we would have to rely on the differences between very few reported experimental values.

Concerning the systems in the X23 set, Roux et al.[74] have analysed the experimental measurements for aromatic hydrocarbons and estimate the error in their recommended sublimation enthalpy to be 0.2, 0.3, and 1.3 kJ mol^{-1} for benzene, naphthalene, and anthracene, respectively. Emelyanenko et al.[75] have estimated the error for cytosine to be 2.0 kJ mol^{-1}. As worst-case scenario, for 1,4-cyclohexanedione and adamantane, the maximum deviation between two experiments is 9 and 10 kJ mol^{-1}, respectively. As the average of the experimentally available data is typically used as reference, we can assume that the error in the experimental sublimation enthalpies can become as large as 5 kJ mol^{-1} in certain cases.

The effect of thermal expansion is completely neglected in the harmonic approximation. Therefore, we also investigate the importance of anharmonic effects for the reference values of

lattice energies. We have obtained thermally expanded unit cells corresponding to T_h^{calc} via the QHA using PBE+D3. This allows us to determine the change in lattice energy upon thermal expansion ($\Delta\Delta E_{latt}^{QHA}$) and the corresponding modification of the vibrational energy ($\Delta\Delta E_{vib}^{QHA}$). Both terms are listed in Table S8 (ESI†) and are aggregated to $\Delta\Delta E_{sub}^{QHA}$ (see Table 4), which describes the total effect of including thermal expansion into the description of sublimation enthalpies. Based on eqn (14), we have derived a second set of reference values ($E_{latt}^{ref,QHA}$), which is shown in Table 5. It can be seen that accounting for thermal expansion within the QHA leads to an average modification of reference values by only 1.6 kJ mol^{-1}. In comparison, the average of all $\Delta E_{vib} + 4RT$ terms amounts to 6 kJ mol^{-1}. This implies that the corrections for the sublimation enthalpies ($\Delta E_{vib} + 4RT + \Delta\Delta E_{sub}^{QHA}$) are in all cases closer to the semi-anharmonic values of Reilly and Tkatchenko[31] compared to $\Delta E_{vib} + 4RT$.

Furthermore, in order to evaluate the quality of the used QHA, we derive a third set of reference values ($E_{latt}^{ref,exp}$) by utilizing experimental unit-cell volumes and experimental heat capacities when available (see Table S1, ESI†). The corresponding correction to the harmonic values is labelled $\Delta\Delta E_{sub}^{exp}$ (see Table 4) and the resulting reference lattice energies are given in Table 5. It can be seen that the $\Delta\Delta E_{sub}^{QHA}$ and $\Delta\Delta E_{sub}^{exp}$ values are in most cases in good agreement having a MAD of only 1.0 kJ mol^{-1}. We observe no systematic differences, as the mean deviation is only 0.1 kJ mol^{-1}. The deviations exceed 2 kJ mol^{-1} for carbon dioxide, hexamine, and imidazole. In the first two cases, these differences originate mainly from the large $\Delta\Delta E_{latt}^{QHA}$ contributions, suggesting that the QHA significantly
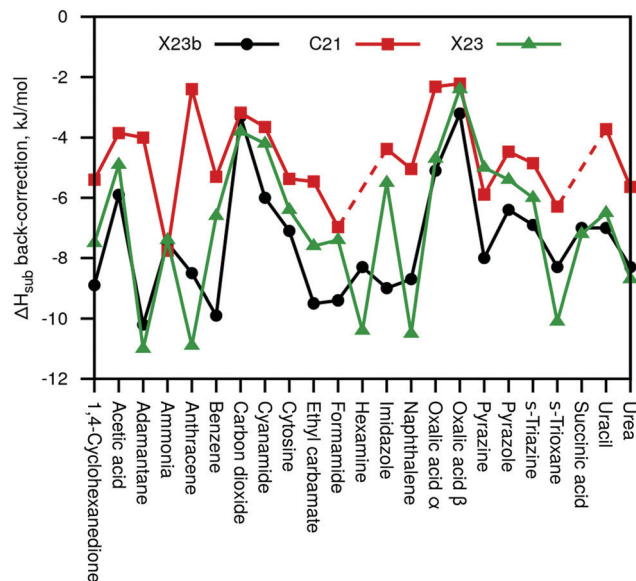
Fig. 3 Calculated sublimation enthalpy back-corrections of our new X23b reference data compared with the back-corrections of the original C21 paper[32] and the X23 paper[31] (including semi-anharmonic values).

overestimates the thermal expansion at T_h^{calc} in these cases. Indeed, for carbon dioxide the QHA leads at 207 K to a thermal expansion (without zero-point energy effects) of 21%, while the experimentally observed thermal expansion between 6 and 205 K amounts to only 9%.[81] Due to this overestimation of the thermal expansion, we believe that the $E_{latt}^{ref,exp}$ reference energies provide a more consistent picture than the $E_{latt}^{ref,QHA}$ values. Therefore, we recommend using the $E_{latt}^{ref,exp}$ reference values, the second last column in Table 5, as new X23b lattice-energy benchmark values. Nevertheless, the QHA is able to yield accurate results in many cases and allows the efficient account for thermal expansion even for large molecular crystals.

Note that we have utilized atom-pairwise dispersion models throughout this paper. As dispersion interactions are not strictly pairwise additive, many-body dispersion interactions can become important for some systems, especially when large and flexible molecules are involved.[82–84] Such interactions can be captured by the many-body dispersion (MBD) model.[85,86] The X23 set, however, involves mainly small and rigid molecules and only small differences between the D3 and MBD dispersion models have been reported.[59,60]

Fig. 3 summarizes the sublimation enthalpy back-corrections of our new X23b ($E_{latt}^{ref,exp}$) reference values compared to the original C21 and X23 values. For C21, we observe a MAD of 2.8 and a maximal deviation of 6.2 kJ mol^{-1}, respectively, compared to the new X23b. Our values agree much better with the X23 reference values (including some anharmonic estimates) with a MAD of 1.4 kJ mol^{-1} and a maximum deviation of 3.5 kJ mol^{-1}. We note that while the new X23b lattice-energy benchmark values are on average rather similar to previous reference data, the maximum deviations are large enough to be of importance for certain systems.

Conclusions

We have derived new reference values of cell volumes and lattice energies for the X23 set of molecular crystals by back-correcting the respective experimental cell volumes and sublimation enthalpies for vibrational contributions. For this purpose, the quasi-harmonic approximation (QHA) was utilized in order to model the thermal expansion of the considered molecular crystals. Based on the average expansion described by three different dispersion-inclusive density functional approximations (PBE+D3, BLYP+D3, and RPBE+D3), we have created a new reference data set for unit-cell volumes, which can be directly compared to lattice relaxations minimizing the electronic energy. This back-correction is crucial and rather large, since it decreased the reference volumes on average by 5% compared to low-temperature experimental values due to zero-point and thermal effects. It has been found that PBE+D3 and BLYP+D3 typically provide a better description of the thermal volumetric expansion compared to high-level estimates than RPBE+D3. Our description of thermal-expansion effects is also more uniform than those typically obtained with empirical force fields.

In the second part, we have focused on the back-correction of sublimation enthalpies for vibrational contributions. First, we have provided a harmonic correction like the one presented by Reilly and Tkatchenko.[31] However, the presented harmonic back-correction herein amounts in all but five cases to the average of our PBE+D3, BLYP+D3, and RPBE+D3 results and the PBE+TS values obtained by Reilly and Tkatchenko. Since we are averaging over three distinct density-functional approximations and two dispersion models (in case of PBE), the resulting reference data is less biased towards the method employed. Furthermore, we have included the change in electronic and vibrational energy due to thermal expansion in our back-correction. In one case, we relied entirely on the QHA, while another back-correction was performed by utilizing experimentally obtained unit-cell volumes and heat capacities. In many cases, these two approaches lead to very similar results, but for a few systems we observe differences exceeding 2 kJ mol^{-1}, which is mainly due to the overestimation of the thermal expansion by the QHA at larger temperatures.

The average effect of thermal expansion for sublimation enthalpies amounts to 1.6 kJ mol^{-1} and is therefore less pronounced than for the unit-cell volumes reported. However, these effects could still be crucial for molecular crystals with complex polymorphic energy landscapes. Note that sublimation enthalpies—in contrast to free energies—do not include entropic effects. Vibrational free energies are mainly determined by low-frequency vibrations, which in turn are modified by the thermal expansion of a crystal. Therefore, the effect of thermal expansion is likely more pronounced for Helmholtz free energies. Moreover, accounting for thermal expansion can be crucial for several properties, for instance low-frequency vibrational spectra or elastic constants.[33]

Since our back-corrections involve the average over several density-functional approximations, we have estimated an uncertainty of our reference values based on the maximal observed

difference from the average. However, the overall accuracy of our new reference data depends on the accuracy of the underlying experimental measurements and used theoretical approximations. For some systems, the error in the underlying experimental sublimation enthalpies can be as large as 5 kJ mol^{-1} and more accurate experimental data would be desirable. Nevertheless, our new revised X23b reference values constitute a consistent high-level estimate and will further enable a more consistent benchmark and development of computational methods for molecular crystals.

Conflicts of interest

There are no conflicts to declare.

Notes and references

1 W. Kohn, *Rev. Mod. Phys.*, 1999, **71**, 1253–1266.
2 J. A. Pople, *Angew. Chem., Int. Ed.*, 1999, **38**, 1894–1902.
3 T. Korona, D. Kats, M. Schütz, T. B. Adler, Y. Liu and H.-J. Werner, in *Linear-Scaling Techniques in Computational Chemistry and Physics: Methods and Applications*, ed. R. Zalesny, M. G. Papadopoulos, P. G. Mezey and J. Leszczynski, Springer, Netherlands, Dordrecht, 2011, pp. 345–407.
4 J. Yang, G. K.-L. Chan, F. R. Manby, M. Schütz and H.-J. Werner, *J. Chem. Phys.*, 2012, **136**, 144105.
5 F. Neese, A. Hansen and D. G. Liakos, *J. Chem. Phys.*, 2009, **131**, 064103.
6 C. Hättig, D. P. Tew and B. Helmich, *J. Chem. Phys.*, 2012, **136**, 204105.
7 S. Saebø and P. Pulay, *J. Chem. Phys.*, 2001, **115**, 3975–3983.
8 J. E. Subotnik, A. Sodt and M. Head-Gordon, *J. Chem. Phys.*, 2006, **125**, 074116.
9 P. Constans, P. Y. Ayala and G. E. Scuseria, *J. Chem. Phys.*, 2000, **113**, 10451–10458.
10 J. C. Burant, M. C. Strain, G. E. Scuseria and M. J. Frisch, *Chem. Phys. Lett.*, 1996, **248**, 43–49.
11 J. Kussmann, M. Beer and C. Ochsenfeld, *Wiley Interdiscip. Rev.: Comput. Mol. Sci.*, 2013, **3**, 614–636.
12 C. A. White, B. G. Johnson, P. M. W. Gill and M. Head-Gordon, *Chem. Phys. Lett.*, 1994, **230**, 8–16.
13 S. Manzer, P. R. Horn, N. Mardirossian and M. Head-Gordon, *J. Chem. Phys.*, 2015, **143**, 024113.
14 E. A. Toivanen, S. A. Losilla and D. Sundholm, *Phys. Chem. Chem. Phys.*, 2015, **17**, 31480–31490.
15 E. Rudberg, E. H. Rubensson and P. Sałek, *J. Chem. Theory Comput.*, 2011, **7**, 340–350.
16 M. A. Watson, Y. Kurashige, T. Nakajima and K. Hirao, *J. Chem. Phys.*, 2008, **128**, 054105.
17 J. J. P. Stewart, *J. Mol. Model.*, 2013, **19**, 1–32.
18 P. O. Dral, X. Wu, L. Spörkel, A. Koslowski, W. Weber, R. Steiger, M. Scholten and W. Thiel, *J. Chem. Theory Comput.*, 2016, **12**, 1082–1096.
19 M. Elstner, D. Porezag, G. Jungnickel, J. Elsner, M. Haugk, T. Frauenheim, S. Suhai and G. Seifert, *Phys. Rev. B: Condens. Matter Mater. Phys.*, 1998, **58**, 7260–7268.
20 L. Maschio, D. Usvyat, M. Schütz and B. Civalleri, *J. Chem. Phys.*, 2010, **132**, 134706.
21 M. Del Ben, J. Hutter and J. VandeVondele, *J. Chem. Theory Comput.*, 2012, **8**, 4177–4188.
22 G. H. Booth, A. Grüneis, G. Kresse and A. Alavi, *Nature*, 2012, **493**, 365–370.
23 S. Suhai and J. Ladik, *J. Phys. C: Solid State Phys.*, 1982, **15**, 4327–4337.
24 A. J. Cruz-Cabeza, S. M. Reutzel-Edens and J. Bernstein, *Chem. Soc. Rev.*, 2015, **44**, 8619–8635.
25 J. P. M. Lommerse, W. D. S. Motherwell, H. L. Ammon, J. D. Dunitz, A. Gavezzotti, D. W. M. Hofmann, F. J. J. Leusen, W. T. M. Mooij, S. L. Price, B. Schweizer, M. U. Schmidt, B. P. van Eijck, P. Verwer and D. E. Williams, *Acta Crystallogr., Sect. B: Struct. Sci.*, 2000, **56**, 697–714.
26 W. D. S. Motherwell, H. L. Ammon, J. D. Dunitz, A. Dzyabchenko, P. Erk, A. Gavezzotti, D. W. M. Hofmann, F. J. J. Leusen, J. P. M. Lommerse, W. T. M. Mooij, S. L. Price, H. Scheraga, B. Schweizer, M. U. Schmidt, B. P. van Eijck, P. Verwer and D. E. Williams, *Acta Crystallogr., Sect. B: Struct. Sci.*, 2002, **58**, 647–661.
27 G. M. Day, W. D. S. Motherwell, H. L. Ammon, S. X. M. Boerrigter, R. G. Della Valle, E. Venuti, A. Dzyabchenko, J. D. Dunitz, B. Schweizer, B. P. van Eijck, P. Erk, J. C. Facelli, V. E. Bazterra, M. B. Ferraro, D. W. M. Hofmann, F. J. J. Leusen, C. Liang, C. C. Pantelides, P. G. Karamertzanis, S. L. Price, T. C. Lewis, H. Nowell, A. Torrisi, H. A. Scheraga, Y. A. Arnautova, M. U. Schmidt and P. Verwer, *Acta Crystallogr., Sect. B: Struct. Sci.*, 2005, **61**, 511–527.
28 G. M. Day, T. G. Cooper, A. J. Cruz-Cabeza, K. E. Hejczyk, H. L. Ammon, S. X. M. Boerrigter, J. S. Tan, R. G. Della Valle, E. Venuti, J. Jose, S. R. Gadre, G. R. Desiraju, T. S. Thakur, B. P. van Eijck, J. C. Facelli, V. E. Bazterra, M. B. Ferraro, D. W. M. Hofmann, M. A. Neumann, F. J. J. Leusen, J. Kendrick, S. L. Price, A. J. Misquitta, P. G. Karamertzanis, G. W. A. Welch, H. A. Scheraga, Y. A. Arnautova, M. U. Schmidt, J. van de Streek, A. K. Wolf and B. Schweizer, *Acta Crystallogr., Sect. B: Struct. Sci.*, 2009, **65**, 107–125.
29 D. A. Bardwell, C. S. Adjiman, Y. A. Arnautova, E. Bartashevich, S. X. M. Boerrigter, D. E. Braun, A. J. Cruz-Cabeza, G. M. Day, R. G. Della Valle, G. R. Desiraju, B. P. van Eijck, J. C. Facelli, M. B. Ferraro, D. Grillo, M. Habgood, D. W. M. Hofmann, F. Hofmann, K. V. J. Jose, P. G. Karamertzanis, A. V. Kazantsev, J. Kendrick, L. N. Kuleshova, F. J. J. Leusen, A. V. Maleev, A. J. Misquitta, S. Mohamed, R. J. Needs, M. A. Neumann, D. Nikylov, A. M. Orendt, R. Pal, C. C. Pantelides, C. J. Pickard, L. S. Price, S. L. Price, H. A. Scheraga, J. van de Streek, T. S. Thakur, S. Tiwari, E. Venuti and I. K. Zhitkov, *Acta Crystallogr., Sect. B: Struct. Sci.*, 2011, **67**, 535–551.
30 A. M. Reilly, R. I. Cooper, C. S. Adjiman, S. Bhattacharya, A. D. Boese, J. G. Brandenburg, P. J. Bygrave, R. Bylsma, J. E. Campbell, R. Car, D. H. Case, R. Chadha, J. C. Cole,

24342 | *Phys. Chem. Chem. Phys.*, 2019, **21**, 24333–24344

This journal is © the Owner Societies 2019

K. Cosburn, H. M. Cuppen, F. Curtis, G. M. Day, R. A. DiStasio Jr., A. Dzyabchenko, B. P. Van Eijck, D. M. Elking, J. A. Van Den Ende, J. C. Facelli, M. B. Ferraro, L. Fusti-Molnar, C. A. Gatsiou, T. S. Gee, R. De Gelder, L. M. Ghiringhelli, H. Goto, S. Grimme, R. Guo, D. W. M. Hofmann, J. Hoja, R. K. Hylton, W. Jankiewicz, D. T. De Jong, J. Kendrick, N. J. J. De Klerk, H. Y. Ko, L. N. Kuleshova, X. Li, S. Lohani, F. J. J. Leusen, A. M. Lund, J. Lv, Y. Ma, N. Marom, A. E. Masunov, P. McCabe, D. P. McMahon, H. Meekes, M. P. Metz, A. J. Misquitta, S. Mohamed, B. Monserrat, R. J. Needs, M. A. Neumann, J. Nyman, S. Obata, H. Oberhofer, A. R. Oganov, A. M. Orendt, G. I. Pagola, C. C. Pantelides, C. J. Pickard, R. Podeszwa, L. S. Price, S. L. Price, A. Pulido, M. G. Read, K. Reuter, E. Schneider, C. Schober, G. P. Shields, P. Singh, I. J. Sugden, K. Szalewicz, C. R. Taylor, A. Tkatchenko, M. E. Tuckerman, F. Vacarro, M. Vasileiadis, A. Vazquez-Mayagoitia, L. Vogt, Y. Wang, R. E. Watson, G. A. De Wijs, J. Yang, Q. Zhu and C. R. Groom, *Acta Crystallogr., Sect. B: Struct. Sci., Cryst. Eng. Mater.*, 2016, **72**, 439–459.

31 A. M. Reilly and A. Tkatchenko, *J. Chem. Phys.*, 2013, **139**, 024705.

32 A. Otero-de-la-Roza and E. R. Johnson, *J. Chem. Phys.*, 2012, **137**, 054103.

33 J. Hoja, A. M. Reilly and A. Tkatchenko, *Wiley Interdiscip. Rev.: Comput. Mol. Sci.*, 2017, **7**, e1294.

34 A. Erba, J. Maul and B. Civalleri, *Chem. Commun.*, 2016, **52**, 1820–1823.

35 J. G. Brandenburg and S. Grimme, *Acta Crystallogr., Sect. B: Struct. Sci., Cryst. Eng. Mater.*, 2016, **72**, 502–513.

36 J. G. Brandenburg, J. Potticary, H. A. Sparkes, S. L. Price and S. R. Hall, *J. Phys. Chem. Lett.*, 2017, **8**, 4319–4324.

37 J. Nyman and G. M. Day, *Phys. Chem. Chem. Phys.*, 2016, **18**, 31132–31143.

38 J. Hoja, H.-Y. Ko, M. A. Neumann, R. Car, R. A. DiStasio Jr. and A. Tkatchenko, *Sci. Adv.*, 2019, **5**, eaau3338.

39 J. Hoja and A. Tkatchenko, *Faraday Discuss.*, 2018, **211**, 253–274.

40 N. Raimbault, V. Athavale and M. Rossi, *Phys. Rev. Mater.*, 2019, **3**, 053605.

41 C. Červinka, M. Fulem, R. P. Stoffel and R. Dronskowski, *J. Phys. Chem. A*, 2016, **120**, 2022–2034.

42 Y. N. Heit and G. J. O. Beran, *Acta Crystallogr., Sect. B: Struct. Sci., Cryst. Eng. Mater.*, 2016, **72**, 514–529.

43 Y. N. Heit, K. D. Nanda and G. J. O. Beran, *Chem. Sci.*, 2016, **7**, 246–255.

44 J. McKinley and G. J. O. Beran, *Faraday Discuss.*, 2018, **211**, 181–207.

45 J. P. Perdew, K. Burke and M. Ernzerhof, *Phys. Rev. Lett.*, 1996, **77**, 3865–3868.

46 A. D. Becke, *Phys. Rev. B: Condens. Matter Mater. Phys.*, 1988, **38**, 3098–3100.

47 C. Lee, W. Yang and R. G. Parr, *Phys. Rev. B: Condens. Matter Mater. Phys.*, 1988, **37**, 785–789.

48 B. Hammer, L. B. Hansen and J. K. Nørskov, *Phys. Rev. B: Condens. Matter Mater. Phys.*, 1999, **59**, 7413–7421.

49 S. Grimme, J. Antony, S. Ehrlich and H. Krieg, *J. Chem. Phys.*, 2010, **132**, 154104.

50 A. D. Becke and E. R. Johnson, *J. Chem. Phys.*, 2005, **123**, 154101.

51 E. R. Johnson and A. D. Becke, *J. Chem. Phys.*, 2005, **123**, 024101.

52 E. R. Johnson and A. D. Becke, *J. Chem. Phys.*, 2006, **124**, 174104.

53 S. Grimme, S. Ehrlich and L. Goerigk, *J. Comput. Chem.*, 2011, **32**, 1456–1465.

54 L. Goerigk, A. Hansen, C. Bauer, S. Ehrlich, A. Najibi and S. Grimme, *Phys. Chem. Chem. Phys.*, 2017, **19**, 32184–32215.

55 G. Kresse and J. Hafner, *Phys. Rev. B: Condens. Matter Mater. Phys.*, 1993, **47**, 558–561.

56 G. Kresse and J. Hafner, *Phys. Rev. B: Condens. Matter Mater. Phys.*, 1994, **49**, 14251–14269.

57 G. Kresse and J. Furthmüller, *Phys. Rev. B: Condens. Matter Mater. Phys.*, 1996, **54**, 11169–11186.

58 G. Kresse and J. Furthmüller, *Comput. Mater. Sci.*, 1996, **6**, 15–50.

59 G. A. Dolgonos, O. A. Loboda and A. D. Boese, *J. Phys. Chem. A*, 2018, **122**, 708–713.

60 O. A. Loboda, G. A. Dolgonos and A. D. Boese, *J. Chem. Phys.*, 2018, **149**, 124104.

61 P. E. Blöchl, *Phys. Rev. B: Condens. Matter Mater. Phys.*, 1994, **50**, 17953–17979.

62 G. Kresse and D. Joubert, *Phys. Rev. B: Condens. Matter Mater. Phys.*, 1999, **59**, 1758–1775.

63 F. D. Murnaghan, *Proc. Natl. Acad. Sci. U. S. A.*, 1944, **30**, 244–247.

64 J. H. Smith and A. I. M. Rae, *J. Phys. C: Solid State Phys.*, 1978, **11**, 1761–1770.

65 R. D. Chirico, S. E. Knipmeyer and W. V. Steele, *J. Chem. Thermodyn.*, 2003, **35**, 1059–1072.

66 A. Togo and I. Tanaka, *Scr. Mater.*, 2015, **108**, 1–5.

67 R. C. Wilhoit, J. Chao and K. R. Hall, *J. Phys. Chem. Ref. Data*, 1985, **14**, 1–175.

68 L. A. K. Staveley, L. Q. Lobo and J. C. G. Calado, *Cryogenics*, 1981, **21**, 131–144.

69 J. B. Hudson, W. B. Hillig and R. M. Strong, *J. Phys. Chem.*, 1959, **63**, 1012–1016.

70 H. G. M. De Wit, C. G. De Kruif and J. C. Van Miltenburg, *J. Chem. Thermodyn.*, 1983, **15**, 891–902.

71 R. M. Stephenson and S. Malanowski, *Handbook of the Thermodynamics of Organic Compounds*, Springer, Netherlands, Dordrecht, 1987.

72 N. Vogt, M. A. Abaev, A. N. Rykov and I. F. Shishkov, *J. Mol. Struct.*, 2011, **996**, 120–127.

73 A. Tkatchenko and M. Scheffler, *Phys. Rev. Lett.*, 2009, **102**, 073005.

74 M. V. Roux, M. Temprado, J. S. Chickos and Y. Nagano, *J. Phys. Chem. Ref. Data*, 2008, **37**, 1855–1996.

75 V. N. Emel'yanenko, D. H. Zaitsau, E. Shoifet, F. Meurer, S. P. Verevkin, C. Schick and C. Held, *J. Phys. Chem. A*, 2015, **119**, 9680–9691.

76 W. Acree and J. S. Chickos, *J. Phys. Chem. Ref. Data*, 2010, **39**, 043101.

This journal is © the Owner Societies 2019

Phys. Chem. Chem. Phys., 2019, **21**, 24333–24344 | **24343**

77 J. F. Martin and R. J. L. Andon, *J. Chem. Thermodyn.*, 1982, **14**, 679–688.

78 P. J. van Ekeren, A. C. G. van Genderen and G. J. K. van den Berg, *Thermochim. Acta*, 2006, **446**, 33–35.

79 A. Togo, L. Chaput, I. Tanaka and G. Hug, *Phys. Rev. B: Condens. Matter Mater. Phys.*, 2010, **81**, 174301.

80 J. Nyman, O. S. Pundyke and G. M. Day, *Phys. Chem. Chem. Phys.*, 2016, **18**, 15828–15837.

81 I. N. Krupskii, A. I. Prokhvatilov, A. I. Erenburg and A. S. Barylnik, *Fiz. Nizk. Temp.*, 1982, **8**, 533–541.

82 A. Ambrosetti, N. Ferri, R. A. DiStasio Jr. and A. Tkatchenko, *Science*, 2016, **351**, 1171–1176.

83 A. Ambrosetti, D. Alfè, R. A. DiStasio Jr. and A. Tkatchenko, *J. Phys. Chem. Lett.*, 2014, **5**, 849–855.

84 A. M. Reilly and A. Tkatchenko, *Chem. Sci.*, 2015, **6**, 3289–3301.

85 A. Tkatchenko, R. A. DiStasio Jr., R. Car and M. Scheffler, *Phys. Rev. Lett.*, 2012, **108**, 236402.

86 A. Ambrosetti, A. M. Reilly, R. A. DiStasio Jr. and A. Tkatchenko, *J. Chem. Phys.*, 2014, **140**, 18A508.